

INTERNATIONAL SYMPOSIUM ON HYDRO- AND AERODYNAMICS IN MARINE ENGINEERING
HADMAR '91
VARNA, BULGARIA, 28 OCTOBER – 1 NOVEMBER 1991
PROCEEDINGS, VOLUME 1, PAPER NO. 5

SHIP BEHAVIOUR AND CONTROL AT LOW SPEED
IN LAYERED FLUIDS

Marc VANTORRE¹
National Fund for Scientific Research
State University of Ghent
Office of Naval Architecture
Grote Steenweg Noord 2
B 9052 GENT-ZWIJNAARDE (BELGIUM)

ABSTRACT

Fluid mud layers on the bottom of navigational channels may affect a ship's behaviour and control.

Tests with self-propelled ship models navigating in a two-layer fluid system have shown the occurrence of an internal undulation system with characteristics depending on the ship's forward velocity.

A simplified one-dimensional theory is developed for determining approximately the interface deformation and the ship's squat.

Results of systematical model tests are discussed. Emphasis is laid on effectivity of propulsion and rudder manoeuvres. There are clear indications for instable rudder behaviour and poor propulsive efficiency if due to a combination of initial keel clearance (KC), squat effects and internal undulations, the ship's keel is in contact with both fluids. The theoretical developments lead to a practical estimation of the conditions in which controllability problems may occur.

NOMENCLATURE

A_i see expression (13)
 B ship's beam
 B_i (local) beam at upper boundary of layer i
 C_i see expression (14)
 C_r see expression (15)
 C_T total resistance coefficient
 D propeller diameter
 F_n Froude number ($= U / (gL)^{1/2}$)
 g gravitational acceleration
 h_i thickness (depth) of layer i
 J' apparent advance ratio
KC keel clearance (relative to interface, in % of draught)
 K_T thrust coefficient ($= T / (\rho_i D^4 n^2)$)
 K_Q torque coefficient ($= Q / (\rho_i D^5 n^2)$)
 L ship's length between perpendiculars
 M total accelerated mass
 m ship's mass
 m_i blockage coefficient of layer i
 N yawing moment
 n number of revolutions of propeller
 O origin (moving with velocity U)
 Q propeller torque
 R resistance
 S_i ship's cross section area wetted by layer i
 S ship's wetted surface

T ship's draught; propeller thrust
 t time; thrust deduction factor
 U ship's forward velocity
 u_i relative horizontal velocity of layer i
 V ship's displacement
 x horizontal coordinate (longitudinal)
 Y lateral force component
 y horizontal coordinate (lateral)
 W channel width
 w wake factor
 Z vertical force component
 z vertical coordinate
 z_i vertical position of upper boundary of layer i
 δ rudder angle
 ζ ship's sinkage
 θ ship's trim
 μ added mass coefficient
 ρ_i mass density of layer i

Subscripts

B buoyancy
crit critical
 J jump
 M model
 m mean
 T total resistance
1,2 referring to fluid layer 1,2

Superscripts

0 referring to situation at rest ($U=0$)
+ positive value
- negative value
* referring to situation without mud
* nondimensional

INTRODUCTION

A ship's performance may be changed substantially if navigating in waters consisting of layers with several densities. The effect of so-called *dead-water*, i.e. a layer of fresh over salt water which e.g. may occur near the mouths of some of the Norwegian fjords, can be mentioned as a well-known, classical example. The abnormal resistance occasionally experienced by ships in such waters is ascribed to waves of considerable height which, owing to the relatively small potential energy involved in a given deformation of the common boundary of both water layers, are easily produced in the interface (see Lamb [1]).

¹ Research Associate; Naval Architect, Ph.D.

Layered fluids may also occur in shallow navigational areas (e.g. approach channels to harbours, harbour areas, inland waterways) if the bottom is covered with fluid mud suspensions. In those cases, difficulties can arise in defining the navigational depth, so that it is necessary to introduce the terms *nautical bottom* and *nautical depth*. A definition of the latter is given in [2]: "the maximum depth ... which, for navigational purposes, is considered safe to accept as the bed of the channel. In arriving at a definition of the bed, the two following criteria need to be met:

- (1) The ship's hull must suffer no damage even if its draft were to reach the full nautical depth.
- (2) The navigational response of the vessel must not be adversely affected."

The knowledge of the physical properties which are typical for this nautical bottom and of the minimum water depth or the minimum KC required for safe navigation is of great importance for design and dimensioning of access channels and harbour basins and for optimization of maintenance dredging work. For this reason, a study program was organized by the Coastal Services of the Ministry of the Flemish Community (Belgium), in order to assure safe navigation and optimal use of the available depth in the approach channels giving access to the ports of Antwerp, Ghent and Zeebrugge. This study is subdivided in two parts (see [3],[4],[5] for details):

- in situ measurements of physico-chemical characteristics of mud layers and execution of full scale navigation and manoeuvring tests;
- ship model test programs to evaluate the effect of a mud layer on a ship's performance in a more systematical way.

The paper will handle some preliminary results of laboratory tests carried out at the Hydraulics Research Laboratory of Borgerhout-Antwerp with self-propelled ship models in a small basin, the bottom of which was covered with a mud-simulating liquid. Many aspects of the ship's behaviour have been investigated; the effect of the presence of a bottom layer appeared to be related to the deformation of the interface between both fluids, the latter depending on the ship's forward velocity. For this reason, it is felt necessary to give a description of the flow in the two-layer system and of the undulation pattern at the interface; a simplified theoretical approach seems to lead to acceptable results. Emphasis is laid on the influence on effectiveness of propulsion and rudder manoeuvres.

EXPERIMENTAL SETUP (see also [5],[6])

Ship models, equipped with propulsion and rudder(s), were forced to follow the centerline of a small basin ($32.0 \times 2.3 \times 0.3 \text{ m}^3$) by means of a guiding beam, but were free to move in vertical direction. A wireless communication system between the ship model and a PC transmitted all signals in a discrete number of equidistant points of the guiding beam. Controlled and measured data are listed in Fig. 1.

The bottom of the tank was covered with 1-1-1 trichloroethane/petrol mixture (TCE/P), which has proved to be the most suitable mud simulating material. The layer thickness was chosen between 11 and 35 mm; typical mass densities were 1110, 1140 and 1220 kg/m³. At one point, vertical interface motions were measured by means of a profile following device.

Two ship models were selected: a LNG-tanker ($267 \times 41.6 \times 11.0 \text{ m}^3$; $C_B = 0.80$; scale 1:70) and a trailing suction hopper dredger ($115.5 \times 23.0 \times 8.0 \text{ m}^3$; $C_B = 0.84$; scale 1:40).

Following tests were carried out with a KC between +20% and -10%:

- acceleration tests (constant rpm);
- deceleration tests (zero rpm);
- steady-state tests (constant $U < 6 \text{ kn}$);
- steady-state tests with rudder action.

VERTICAL INTERFACE MOTIONS

There is a clear relationship between the influence of the presence of a lower fluid layer on the ship's behaviour and the deformation of the interface caused by the pressure field around the moving hull. Model tests have shown that the shape of the interface depends on the ship's speed (see Fig. 2):

- At very low speed, the interface remains practically undisturbed ("first speed range").
- At intermediate speed ("second speed range"), an interface sinkage is observed under the ship's entrance, which at a certain section suddenly changes into an elevation. The section mentioned moves towards the stern with increasing speed. The angle between the jump front and the canal centerline is approximately 90° .
- At higher speed ("third speed range"), the jump occurs aft of the APP; the jump direction grows from 90° to about 135° .

This general pattern is disturbed by secondary internal wave systems if the KC takes small or negative values (Fig. 3).

Some insight into the physical causes of the behaviour of the interface can be acquired by means of a simplified theoretical approach. The problem of the forward motion of a ship with speed U in a canal, the bottom of which is covered with a higher density fluid, is reduced to one of steady flow, in which the ship's position is fixed while the two fluid layers are moving with a velocity $-U$. This flow is disturbed by the presence of the ship's hull, so that the velocities of the fluid layers take values u_1 and u_2 , while the free surface and the interface take vertical positions z_1 and z_2 , respectively. This disturbance is assumed to be constant over a given cross-section.

Continuity of both layers requires (see Nomenclature and Fig. 4 for symbols and conventions):

$$-UWh_1 = u_1 [W(h_1 + z_1 - z_2) - S_1] \quad (1)$$

$$-UWh_2 = u_2 [W(h_2 + z_2) - S_2] \quad (2)$$

If both fluids are assumed to be ideal, Bernoulli's equation yields a boundary condition for dynamic pressure matching on both the interface and the free surface:

$$\frac{1}{2}U^2 = \frac{1}{2}u_1^2 - gz_1 \quad (3)$$

$$\rho_1 \left(\frac{1}{2}u_1^2 + gz_2 \right) - \rho_2 \left(\frac{1}{2}u_2^2 + gz_2 \right) = \frac{1}{2}(\rho_1 - \rho_2)U^2 \quad (4)$$

For given values of the blockage factors m_1 and m_2 , the number of real solutions of the system of four nonlinear equations (1) to (4) with four unknown variables u_1 , u_2 , z_1 and z_2 , depends on the ship's velocity U . At low speed, the system has four sets of real solutions: two of them lead to an interface sinkage, the other ones to an elevation. The difference between the latter decreases with increasing speed and vanishes when the ship's velocity reaches a critical value. If this value is exceeded, no real solutions lead to an interface elevation. Theoretical developments lead to a fair approximation of this critical velocity, [6]:

$$U_{crit}(m_1) = \sqrt{\frac{8}{27} gh_1 \left(1 - \frac{\rho_1}{\rho_2} \right) (1 - m_1)^2} \quad (5)$$

being the maximal velocity at which an elevation of the interface can occur if the blockage of the water layer is m_1 . No elevation can take place at any section if the ship's speed exceeds following value:

$$U_{crit}(0) = \sqrt{\frac{8}{27} gh_1 \left(1 - \frac{\rho_1}{\rho_2} \right)} \quad (6)$$

The theory explains why interface elevations under the ship's hull can only take place at low speed, but gives neither an explanation for the jump phenomenon, nor an indication for the position x_j of the jump. In order to give an approximation for the latter, it is supposed that the volume of the lower fluid

layer is constant (see fig. 5) :

$$\begin{aligned} & \int_{-\frac{1}{2}L}^{\frac{1}{2}L} (W z_2(x) - S_2(x)) dx \\ & = \int_{-\frac{1}{2}L}^{x_2} (W z_2^+(x) - S_2(x)) dx + \int_{x_2}^{\frac{1}{2}L} (W z_2^-(x) - S_2(x)) dx \\ & = 0 \end{aligned} \quad (7)$$

where $z_2^+(x)$ and $z_2^-(x)$ denote the possible values for interface elevation (>0) and sinkage (<0) at section x , respectively. As vertical ship motions due to squat effects (see further) and the vertical interface position z_2 need to be taken into account for the determination of $S_2(x)$, x_2 needs to be calculated iteratively.

Figs. 2, 3, 6 and 7 give a comparison between measured and calculated values for interface elevation and sinkage and for the position of the jump. Substantial differences only occur at very low speed, where the theory leads to unrealistically large values for the interface sinkage.

VERTICAL SHIP MOTIONS (SQUAT)

Calculation method.

The vertical buoyancy force $Z_B(x)$ acting on the ship's section at coordinate x is given by :

$$Z_B(x) = g(\rho_1 S_1(x) + \rho_2 S_2(x)) \quad (8)$$

The situation at zero speed is chosen as a reference :

$$\begin{aligned} Z(x) &= g[\rho_1(S_1(x) - S_1^0) + \rho_2(S_2(x) - S_2^0)] \\ &= g\rho_1[S(T - \zeta + z_1) - S(T)] + g(\rho_2 - \rho_1)(S_2 - S_2^0) \\ &= g\rho_1 B_1(z_1 - \zeta) + g(\rho_2 - \rho_1)(S_2 - S_2^0) \end{aligned} \quad (9)$$

where $\zeta(x)$ denotes the local vertical position of the ship at section x :

$$\zeta(x) = \zeta_m + \theta x \quad (10)$$

ζ_m and θ being the mean sinkage and trim, respectively. The condition of static equilibrium yields expressions for ζ_m and θ :

$$\zeta_m = \frac{C_7 A_2 - C_1 A_1}{A_2 A_2 - A_1^2} \quad (11)$$

$$\theta = \frac{C_1 A_2 - C_2 A_1}{A_2 A_2 - A_1^2} \quad (12)$$

where

$$A_n = \int_{-\frac{1}{2}L}^{\frac{1}{2}L} B_1 x^n dx \quad (13)$$

$$C_n = \int_{-\frac{1}{2}L}^{\frac{1}{2}L} B_1 z_1 + \left(\frac{\rho_2}{\rho_1} - 1\right)(S_2 - S_2^0) x^n dx \quad (14)$$

If the vertical motion of the ship is related to the initial situation in which no contact occurs between the hull and the lower (mud) layer, C_n needs to be replaced with C_n^* in expressions (11) and (12) :

$$C_n^* = \int_{-\frac{1}{2}L}^{\frac{1}{2}L} B_1 z_1 + \left(\frac{\rho_2}{\rho_1} - 1\right) S_2 x^n dx \quad (15)$$

Sinkage and trim defined in this way are denoted ζ_m^* and θ^* .

Characteristic velocities (fig. 8).

Due to vertical motions of interface and ship, the relative position between both depends on the ship's speed. For each bottom configuration and initial KC several speed ranges can be defined, separated by a number of characteristic velocities :

- (1) the velocity at which contact occurs between the hull (keel) and the rising part of the interface;
- (2') the maximum velocity at which elevation of the interface can occur at the parallel middle body;
- (2'') the maximum velocity at which elevation of the interface can occur at any section;
- (3) the velocity at which local contact occurs between the hull and the sinking interface;
- (4) the velocity at which the keel is completely flooded by the sinking part of the interface;
- (5) the velocity at which contact occurs between the hull and the solid bottom.

For a given ship navigating above a particular bottom, these characteristic velocities can be plotted as a function of KC (fig. 9). According to the type of contact between the keel and the lower fluid layer, several zones can be defined :

no shading :	no contact
vertical shading :	contact with rising interface
interrupted horizontal shading :	contact with sinking interface
horizontal shading :	full contact

Note : the theoretical curve (4a) should be replaced by the experimental curve (4b) in the very low speed range.

Discussion

Fig. 10 shows some results of theoretical calculations of sinkage and trim. If the KC is sufficiently large, the elevation of the interface occurring under the stern in the second speed range will cause a trim by the bow and a slightly larger mean sinkage compared with a solid bottom situation. With decreasing KC, contact takes place between keel and interface. The vertical force on the aft part of the ship, which is initially directed downwards, will decrease in absolute value and even change its sign, causing the sinkage to decrease and even change into an elevation, and trimming the ship by the stern.

In the third speed range, squat effects are generally smoothened compared with the solid bottom situation, particularly if contact occurs between the lower layer and the keel.

The agreement between experimental and theoretical values for the mean sinkage and trim is quite satisfactory. Differences are, presumably due to neglect of propeller effects, more important for the trim angle values, but theory and experiment reveal comparable trends (see fig. 11).

RESISTANCE AND PROPULSION

Experimental results.

Introduction. As a well-equipped towing carriage was not (yet) available, it is not possible to produce precise, quantitative conclusions concerning resistance and propulsion characteristics. Nevertheless, the results of the systematic test series lead to qualitative considerations. Following data are available :

- relation rpm - speed in steady-state situation;
- deceleration of the model with zero rpm;
- thrust (and torque) in steady-state.

Relation rpm-speed. The relation between the number of revolutions of the propeller(s) and the forward velocity appears to be nearly linear for a ship navigating above a solid bottom. Fig. 12 shows that this linear relationship is disturbed by the presence of a lower fluid layer : in the second speed range, the velocity decreases substantially. The effect is much smaller or even negligible in the first and third speed ranges.

The transition between second and third speed range is smoothened with decreasing KC: at very low (negative) KC, the rpm-speed curve is again almost linear.

Deceleration tests. If the propeller rate of revolution is zero, only resistance and inertia forces act on the ship model :

$$R + M \frac{dU}{dt} = 0 \quad (16)$$

where R is the total resistance,

$$R = \frac{1}{2} \rho_1 U^2 S C_T \quad (17)$$

and M denotes the total accelerated mass :

$$M = (1 + \mu_x) m \quad (18)$$

so that the coefficient for total resistance can be written as :

$$C_T = - (1 + \mu_x) \frac{m}{\frac{1}{2} \rho_1 S} \frac{\frac{dU}{dt}}{U^2} = - (1 + \mu_x) \frac{2 \nabla}{S} \frac{\frac{dU}{dt}}{U^2} \quad (19)$$

If the added mass coefficient is considered as a constant, $(dU/dt) + U^2$ is proportional to the resistance coefficient.

Some results are shown in fig. 13. The resistance coefficient increases in a well-defined velocity range, and suddenly decreases at a particular speed value. The effect is smoothened with decreasing KC . For positive KC , the resistance coefficient reaches its maximum at the speed value given by (1) in fig. 8-9, being the speed at which contact occurs between the rising part of the interface and the keel. At very low and relatively high speed, the effect of the lower fluid layer is rather restricted.

Thrust and torque coefficients. Thrust and torque on the propeller shafts were measured during the tests with the model of the suction hopper dredger. However, the available experimental facilities did not allow measurement of the speed of advance. For this reason, thrust and torque coefficients K_T and K_Q are plotted as functions of the apparent advance ratio :

$$J' = \frac{U}{nD} \quad (20)$$

Some typical examples are given in fig. 14. The presence of an interface appears to yield higher values for K_T and K_Q , except for large J' ; this suggests an increase of the wake factor.

The curves show some irregularities if the rising part of the interface is situated near the stern, which occurs at velocities between curves (6) and (2) in fig. 9. The nature of these irregularities seems to depend on transient phenomena. In case of a steady state in the speed range mentioned above, the values of K_T and K_Q are comparable with bollard pull situations; on the other hand, if the speed range is frequented during acceleration, the curves only show some oscillations.

Thrust and resistance. In fig. 15, the thrust on the propellers is represented as follows :

$$\frac{T}{\frac{1}{2} \rho_1 S U^2} = \frac{C_T}{1 - t} \quad (21)$$

which allows a comparison with the results of deceleration tests

$$- \frac{2 \nabla}{S} \frac{\frac{dU}{dt}}{U^2} = \frac{C_T}{1 + \mu_x} \quad (22)$$

A value for $(1 - t) + (1 + \mu_x)$ is calculated; it should be mentioned that these results are only suitable for qualitative study. If the added mass coefficient is considered as a constant, following conclusions can be drawn :

- the thrust deduction factor t decreases if an interface elevation takes place under a considerable fraction of the aft body;
- t increases if the interface jump is concentrated at the stern and contact occurs between keel and lower fluid.

The second conclusion is affirmed by the increase of the wake factor w in the velocity range considered.

Discussion.

The question arises whether the "hollow" in the $U(n)$ -curve is caused by an increase of resistance, or by a decrease

of propulsion efficiency. As a matter of fact, the results of deceleration tests show that the resistance coefficient reaches its maximum at a velocity which is lower than the value corresponding with this hollow.

The influence of the existence of an interface on resistance can be explained as follows. A sinkage of the interface will increase the relative speed between the lower layer and the ship, while the velocity of the ship through the water will slightly decrease compared with the solid bottom situation (fig. 16a). This means that an interface sinkage only leads to an increase of frictional resistance if contact takes place between the keel and the lower layer (fig. 16b).

On the other hand, an interface elevation will reduce the relative motion of the lower fluid, and increase the relative water velocity. If no contact takes place between the hull and the lower fluid (fig. 16c), the occurrence of an interface jump under the keel will increase the relative velocity and, as a consequence, the frictional resistance. In spite of the higher viscosity of the lower fluid, contact between the rising interface and the keel (fig. 16d) will not necessarily cause an increase of resistance. As the relative velocity of the lower layer is considerably lower than the relative water velocity, even a global reduction of frictional resistance can take place. This fact is affirmed by simplified calculations for a qualitative resistance estimation, based on the interface registrations, [7].

This leads to the conclusion that the shape of the $U(n)$ -curve is mainly caused by the influence of interface motions on the propulsion characteristics. If contact occurs between the rising interface and the after body, indications are that the flow through the propeller is obstructed, causing an increase of both thrust deduction and wake factors. Although practical conclusions cannot be derived in this early stage of research, difficulties might occur concerning ship control if the interface jump is concentrated near the stern. The reduction of propulsion efficiency in combination with the relatively low resistance might e.g. increase stopping distance in these circumstances.

RUDDER FORCES

Forces induced on the hull by rudder action have been measured and plotted in a nondimensional way as a function of the rudder angle δ . Above a solid bottom, a rudder command to port generates a lateral force Y on the rudder pointing to starboard, resulting into a moment N forcing the ship to yaw to port. As a consequence, the $Y'(\delta)$ - and $N'(\delta)$ -curves are characterized by a negative and a positive slope, respectively. The curves resulting from tests above TCE/P do not always follow this pattern. In some cases, Y' and N' only take the usual sign for large rudder angles (e.g. $\delta > 20^\circ$); for small δ , the forces induced by rudder action are pointing to the opposite direction. This phenomenon will be called "instability of rudder action".

Sometimes instability is observed for lateral force only, the yawing moment taking the normal sign. This means that although Y takes the wrong sign, the ship is turned to the right direction, as the application point is situated in the fore body.

A clear relationship is observed between interface motions and rudder action stability.

- If the interface jump is situated near midships, restricted instability of the lateral force can occur if contact takes place between the keel and the rising part of the interface (between (1) and (2') on fig. 9); rudder action regains its stability if the keel is permanently flooded by the lower layer ($-4\% < KC < 10\%$ in the situation of fig. 17a).
- If the jump is situated under the aft body, strong instability of both Y and N occur in a rather large KC range (-4% to 10% in fig. 17b), where contact takes place between keel and both layers (fig. 9, between (2') and (2'')).

- At higher velocities, rudder action shows a slight instability at negative KC (-4% in fig. 17c).

It is clear that instable rudder action takes place if the keel is in contact with both water and mud, especially when the contact zone with the lower fluid is situated near the stern.

CONCLUSIONS

It is clear that definitive, quantitative conclusions about the effect of the presence of mud layers on ship controllability can only be based on captive resistance and manoeuvring tests performed in a well-equipped model basin.

Nevertheless, the present results yield some clear indications. A strong relationship is observed between the modifications which ship behaviour and controllability may undergo when navigating in muddy areas and the relative motion between interface and ship hull. The effect of mud layers reaches a maximum in a restricted speed range, the upper limit of which is given by (6), if the initial keelclearance is small enough to allow contact between the hull and the mud layer. There are strong indications for reduction of controllability of both rudder and propulsion in these circumstances.

Practice has shown that it is possible to navigate safely with restricted or even negative KC in muddy waterways. However, it is necessary for pilots to be aware of the effects of layered fluids hydrodynamics. For this reason, a systematic program will be executed in the shallow water towing and manoeuvring tank which is now under construction at the Hydraulic Research Laboratory of Antwerp-Borgerhout. It is the purpose to use the test results as input data for real-time manoeuvring simulator tests.

ACKNOWLEDGEMENTS

This study of the behaviour of mud layers and of ships moving above them is organized by the Coastal Service (Ostend) of the Ministry of the Flemish Community (Environment and Infrastructure). Model tests were carried out at the Hydraulic Research Laboratory (Antwerp-Borgerhout) of the same Ministry, scientifically supported by the Office of Naval Architecture (University of Ghent) and the Belgian National Fund for Scientific Research. Full-scale tests were executed with a vessel of Overseas Decloedt NV by the study-group TV Optimalisatiestudie (Zeebrugge) and Haecon NV (Ghent).

REFERENCES

- [1] Lamb H. Hydrodynamics. Dover Publications, New York, 1932.
- [2] Navigation in muddy areas. Permanent Technical Committee II - Report of Working Group No. 3a. PIANC-Bulletin No. 43, 1982-1983, pp. 21-28.
- [3] Kerckaert P., Malherbe B., Bastin A. Navigation in muddy areas - The Zeebrugge experience. PIANC Bulletin No. 48, 1985, pp. 127-135.
- [4] Kerckaert P., Vandenbossche D., Malherbe B., Druyts M., Van Craenenbroeck K. Maintenance dredging at the port of Zeebrugge : procedures to achieve an operational determination of the nautical bottom. KVIV, 9th International Harbour Congress, Antwerp, 1988, pp. 4.13-32.
- [5] Wens F., De Wolf P., Vantorre M., De Meyer C. A hydro-meteo system for monitoring shipping traffic in narrow channels in relation with the problem of the nautical bottom in muddy areas. PIANC, 27th International Navigation Congress, Osaka, 1990, S. II-1, pp. 5-16.
- [6] Vantorre M., Coen I. On sinkage and trim of vessels navigating above a mud layer. KVIV, 9th International Harbour Congress, Antwerp, 1988, pp. 4.149-161.
- [7] Lasure K. Influence of fluid mud on a ship's resistance and propulsion (graduate thesis; in Dutch). State University of Ghent, 1989.

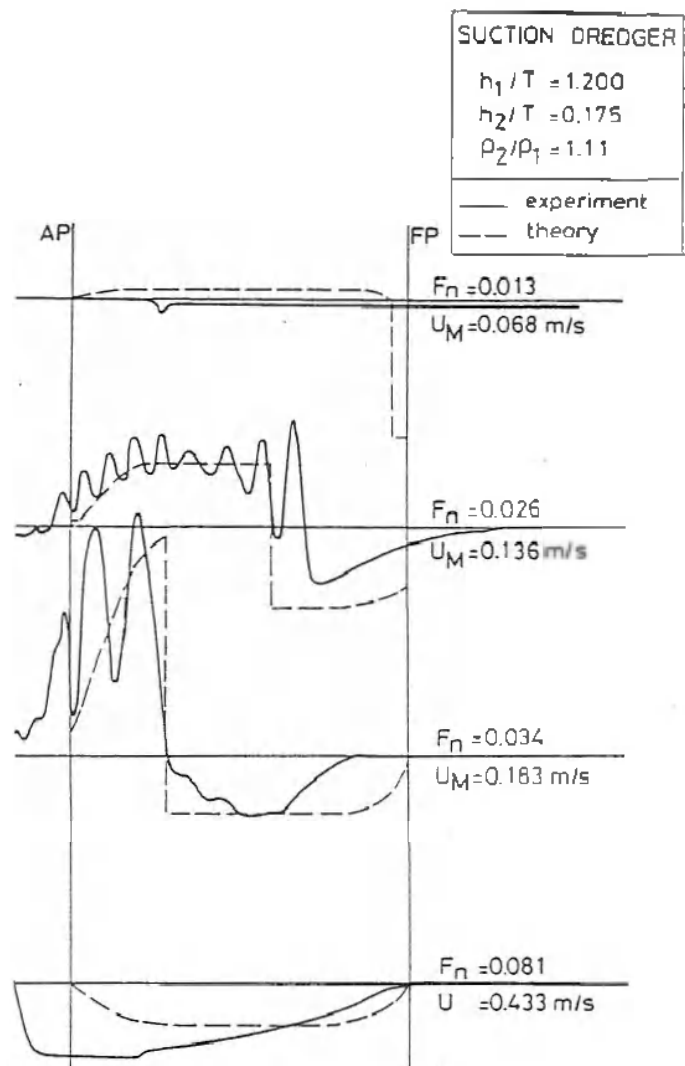


Figure 2. Vertical interface motions : influence of speed.

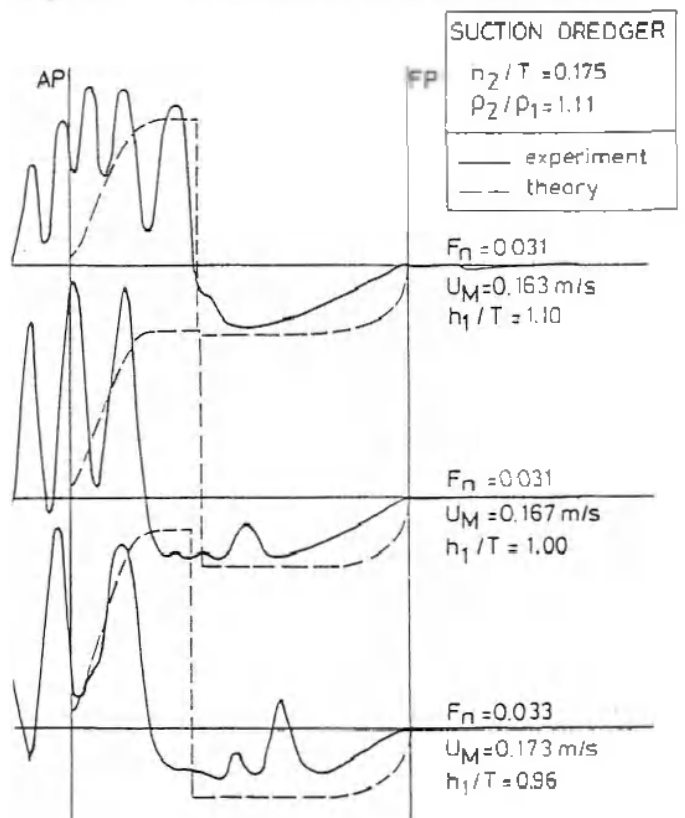


Figure 3. Vertical interface motions : influence of KC.

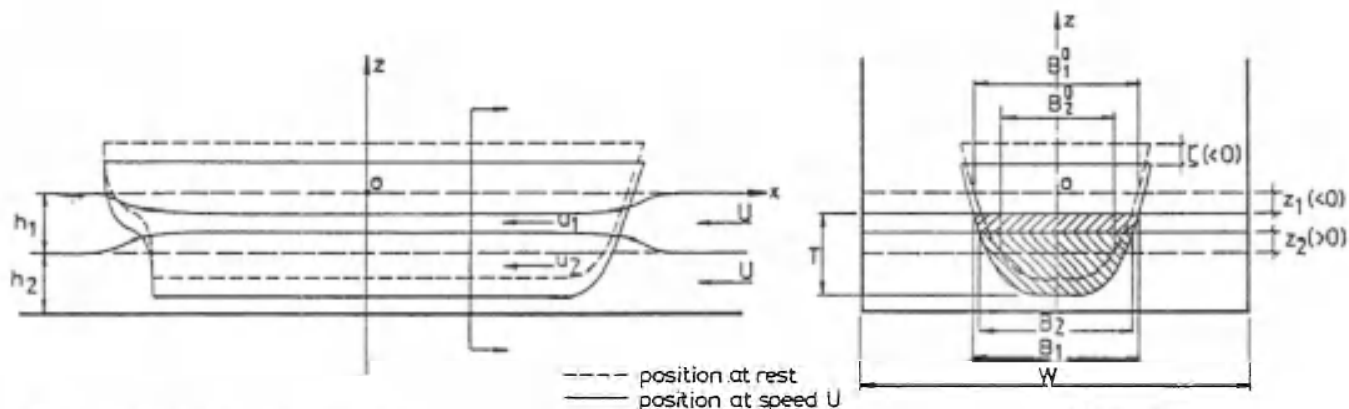


Figure 4. Symbols and conventions.

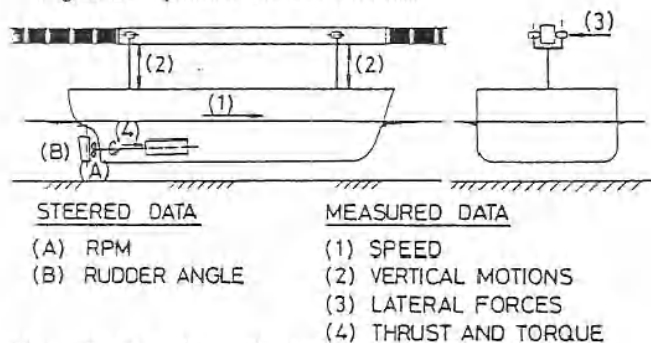


Figure 1. Experimental setup.

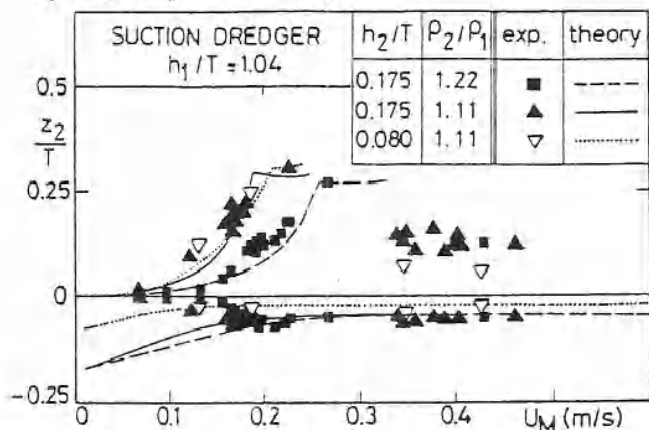


Figure 7. Extremal vertical interface motions (theory and experiment).

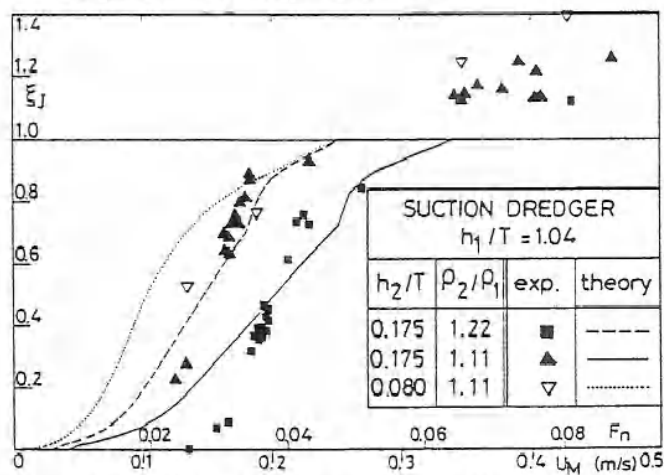


Figure 6. Position of interface jump : influence of bottom configuration (theory and experiment).

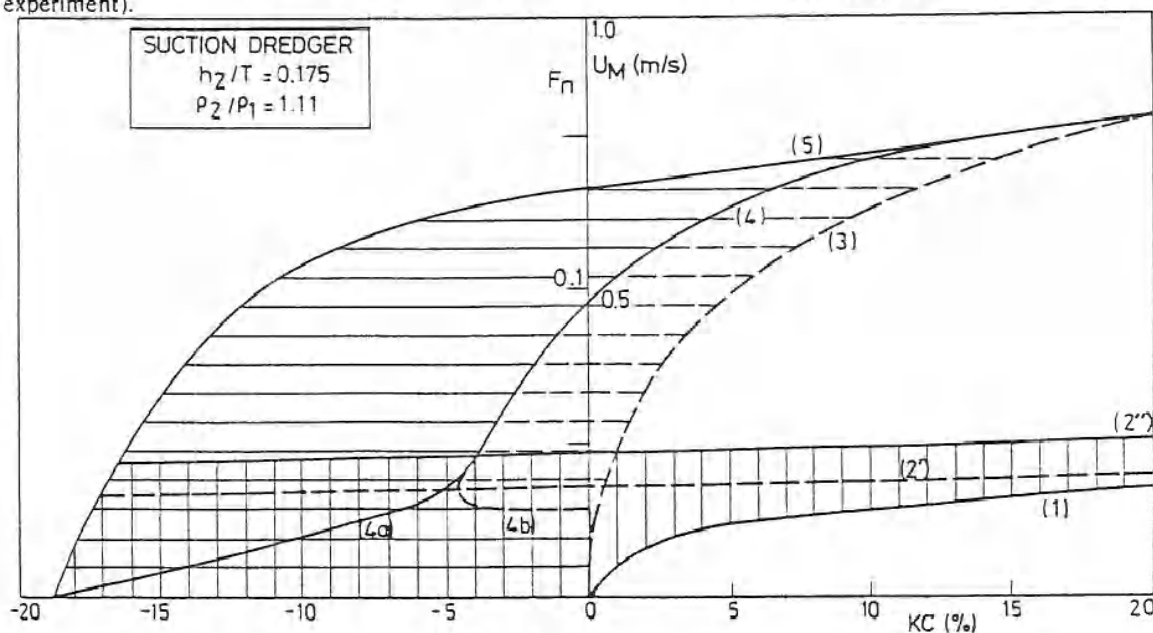


Figure 9. Characteristic velocities vs. KC (theory).

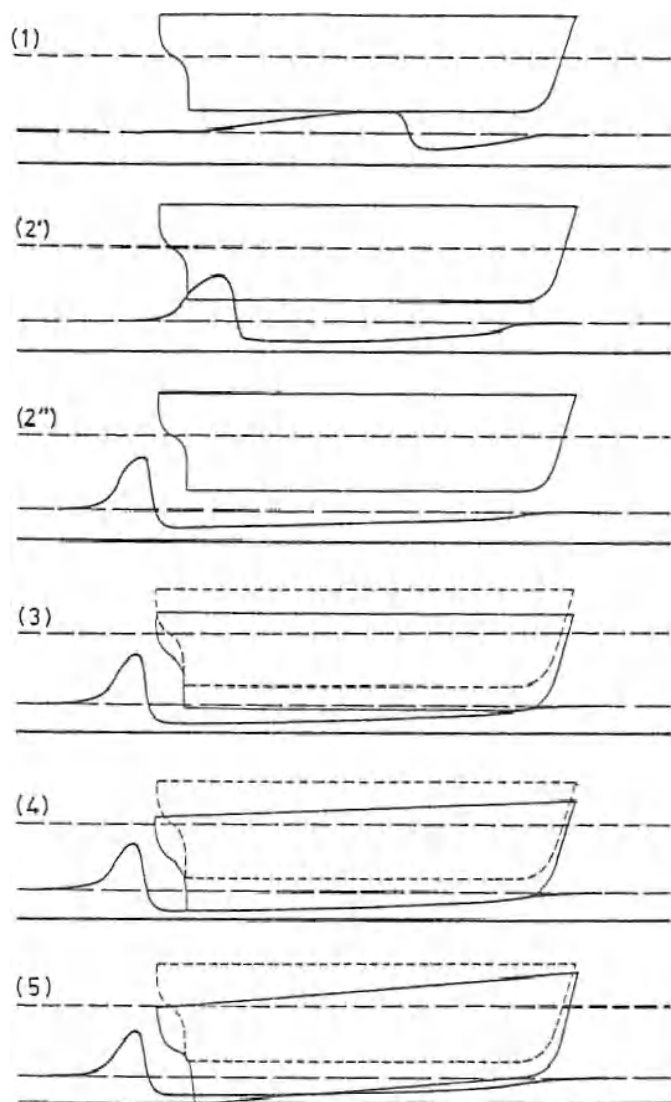


Figure 8. Characteristic velocities.

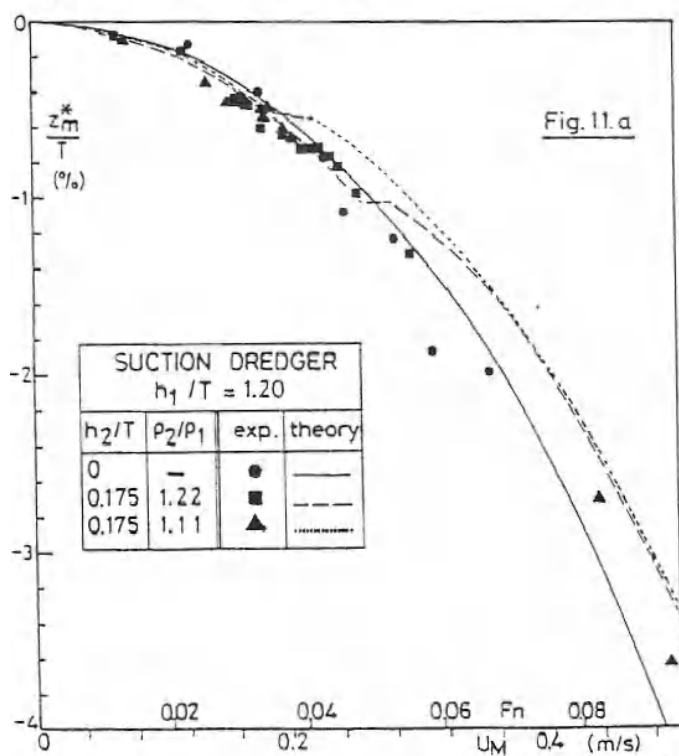


Figure 11. Average sinkage and trim : influence of bottom configuration (theory and experiment).

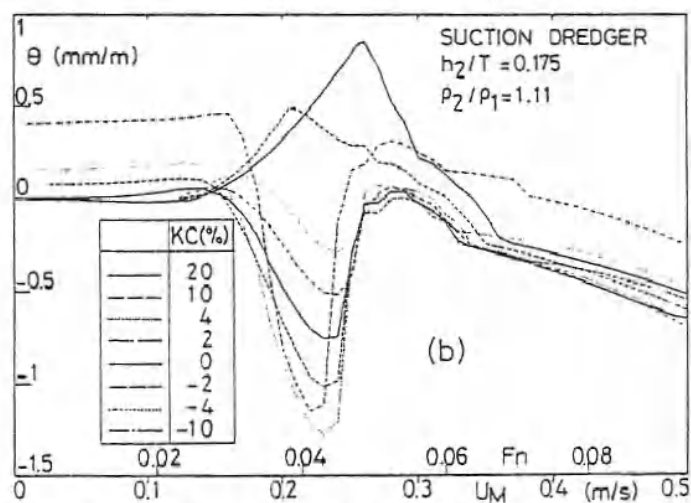
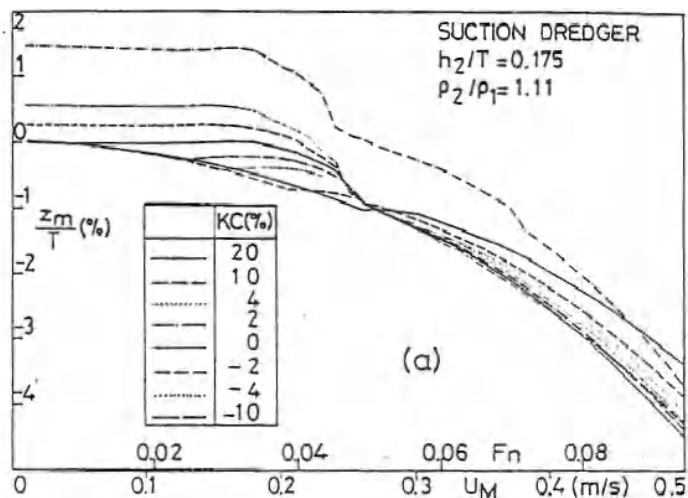
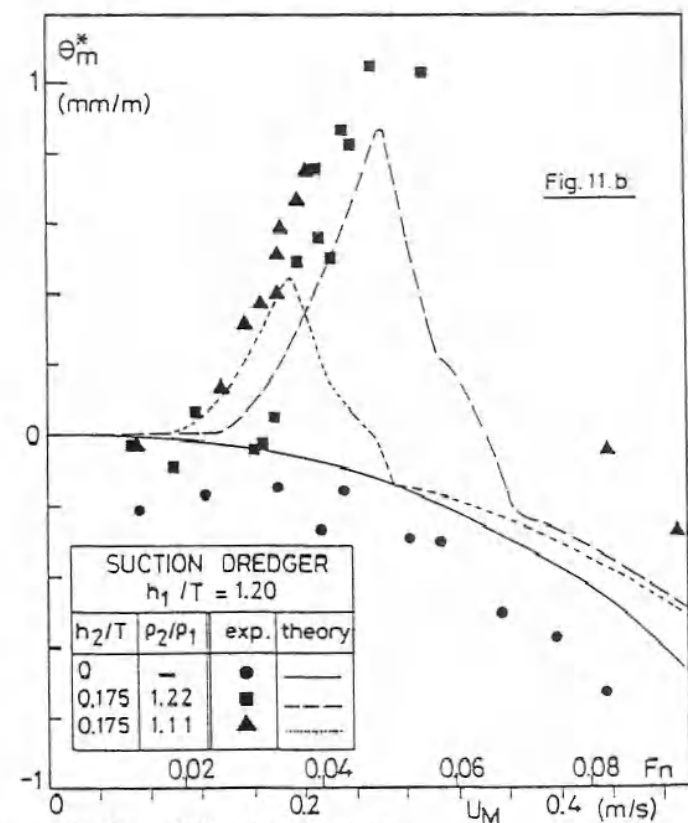


Figure 10. Average sinkage and trim: influence of KC (theory).



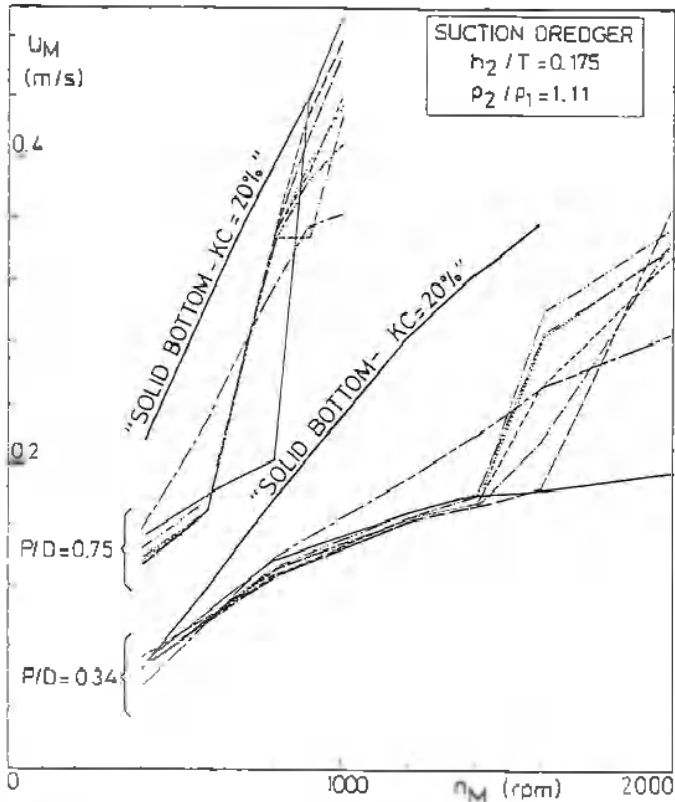
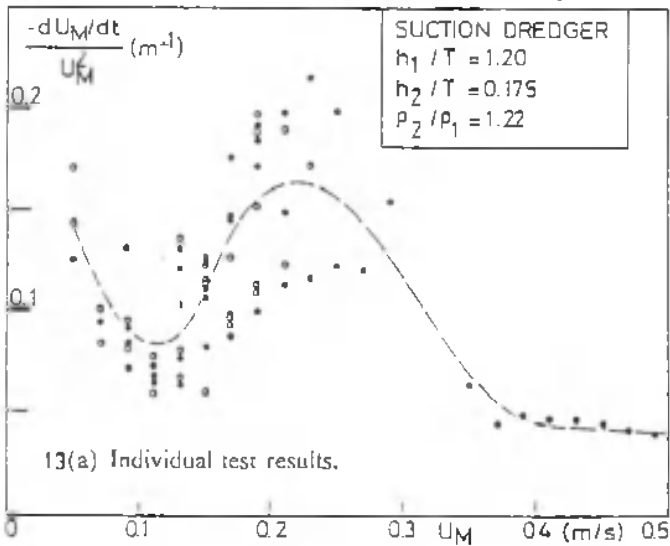
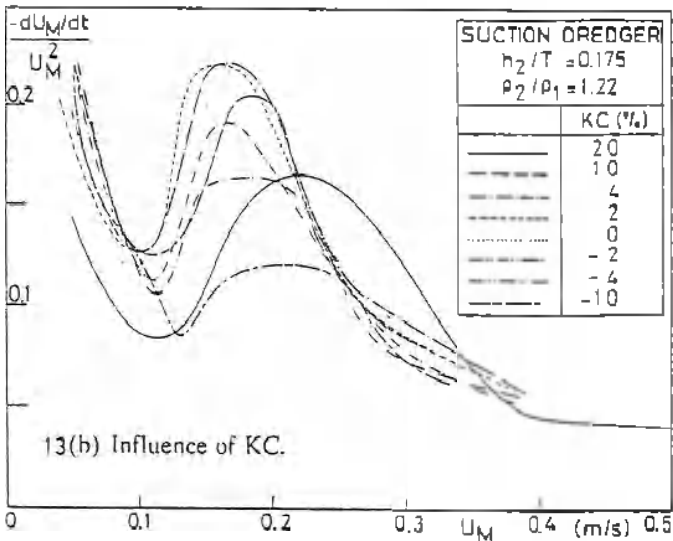


Figure 12. Speed-rpm relation : influence of KC (experiment).



13(a) Individual test results.



13(b) Influence of KC.

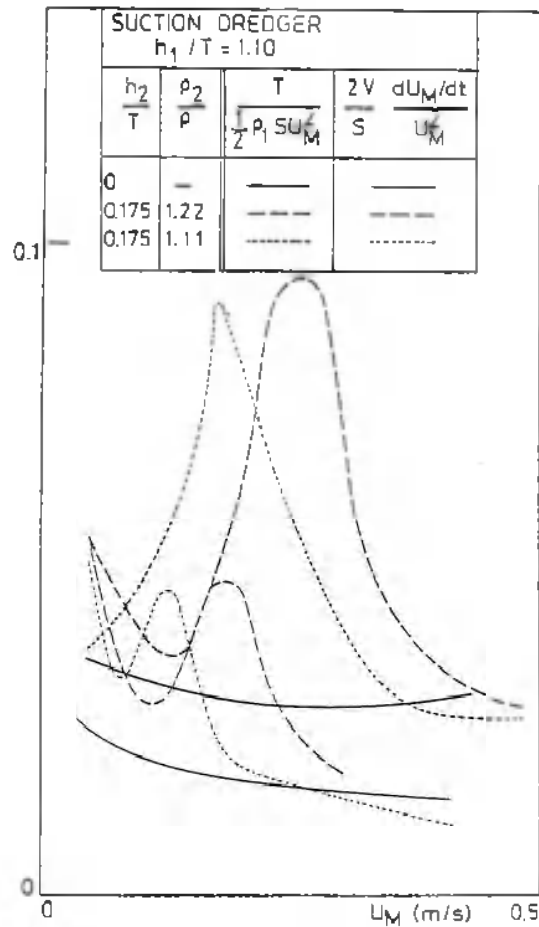


Figure 13. Undimensioned thrust and deceleration vs. speed : influence of bottom configuration (experiment).

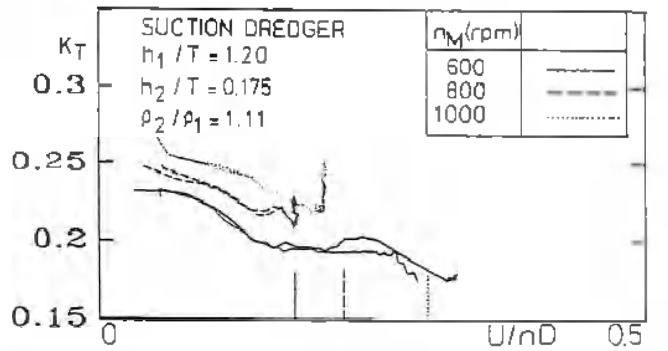


Figure 14. Thrust coefficient vs. apparent speed of advance (experiment). Marked abscissae correspond with respective critical speed values (6).

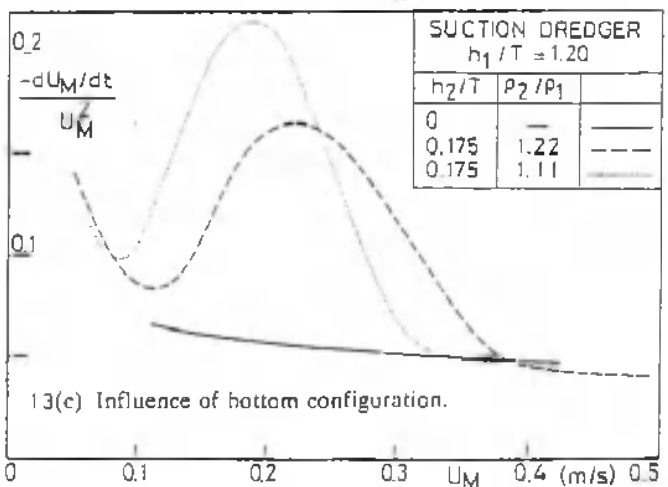


Figure 13. Deceleration tests : $(dU/dt) \div U^2$ vs. speed.

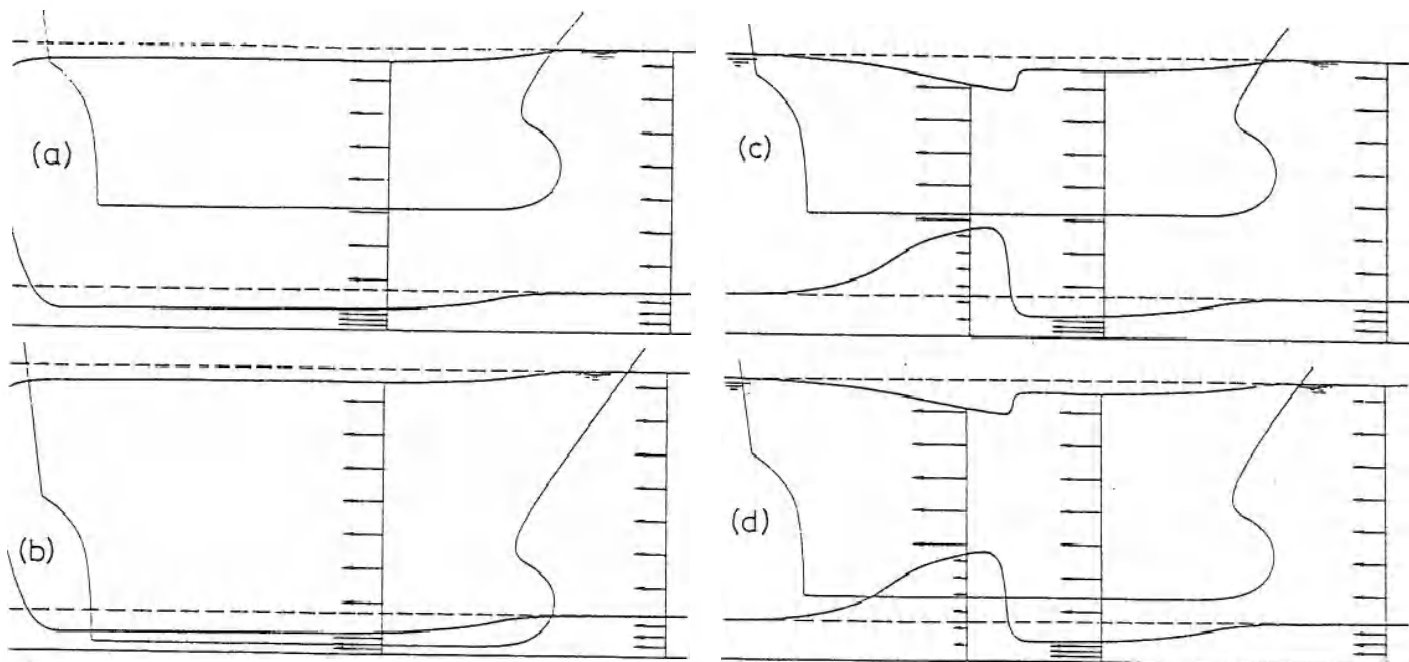


Figure 16. Flow around a ship navigating in a two-layer system.

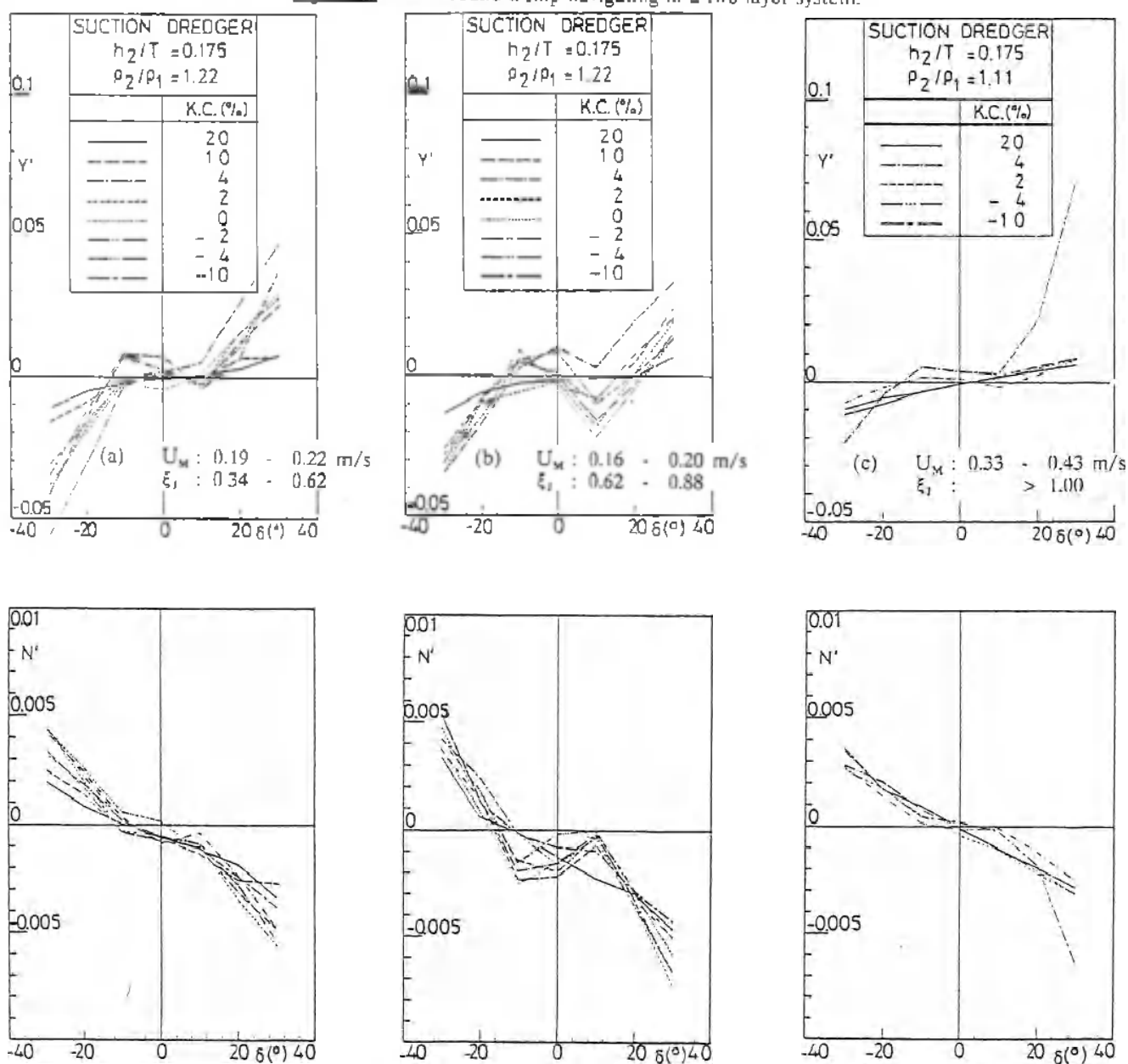


Figure 17. Rudder action : influence of KC and interface jump position (experiment).